Technical Briefs

Modeling and Multivariable Control Design Methodologies for Hexapod-Based Satellite Vibration Isolation

Alok Joshi

Won-jong Kim
e-mail: wjkim@tamu.edu

Department of Mechanical Engineering,
Texas A&M University,
College Station,
Texas 77843-3123, USA

A mathematical model of a six-degree-of-freedom (6-DOF) hexapod system for vibration isolation was derived in the discrete-time domain on the basis of the experimental data obtained from a satellite. Using a Box–Jenkins model structure, the transfer functions between six piezoelectric actuator input voltages and six geophone sensor output voltages were identified empirically. The 6×6 transfer function matrix is symmetric, and its off-diagonal terms indicate the coupling among different input/output channels. Various multi-input multi-output (MIMO) control techniques such as Linear Quadratic Gaussian and H^∞ were proposed for active vibration isolation in the broadband up to 100 Hz. The simulation results using these controllers obtain 13 and 8 dB vibration attenuation at 25 and 35 Hz, respectively.
[DOI: 10.1115/1.2101842]

1 Introduction

A hexapod is a parallel-actuated, closed-chain kinematic structure. It is an isostatic mechanism based on six variable-length struts with six independent linear actuators, interconnected with lower and upper mounting plates. It allows 6-DOF control for positioning of the upper mounting plate. The hexapod structure has gained more popularity in many applications in the last decade including next-generation machine tools [1,2], space structure positioning, and pointing in programs such as the International Space Station [3], active optics [4], and six-axis vibration isolation [5].

Mathematical modeling of a 6-DOF hexapod system can be done in several ways. The Newton–Raphson method with first-

order gradient correction for calculation of the Jacobian and inverse Jacobian, the One Point Iteration method or Homotopy method can be used for closed-form kinematics solutions for hexapod systems [6,7]. In this paper we use a system identification approach for the estimation of the transfer function matrix relating six actuator inputs to the six geophone outputs for the hexapod system.

For mathematical modeling of the hexapod, we refer to the specific geometric details of a hexapod system used in the "Satellite UltraQuiet Isolation Technology Experiment (SUITE)" [8]. SUITE has been selected by the Air Force Space and Missile Center (SMC) and Space Test Program (STP) office for a flight on the PICOSatellite. The objective of SUITE is to provide a quiet platform for precision sensors on a noisy spacecraft. We developed algorithms for vibration isolation through the SUITE Guest Investigator Program at the Air Force Research Laboratory. For broadband and narrow-band active vibration isolation, methods such as direct adaptive disturbance rejection, robust adaptive filtering algorithms using smart materials have been used. The treatment of the hexapod assembly as a combination of six decoupled single-input single-output (SISO) systems have also been used [9,10]. The main objective of this research is to model a 6-DOF hexapod and reduce vibration in the broadband of 5 to 100 Hz.

In this paper, we first describe the SUITE hardware and software. System identification using a chirp signal and bandlimited white Gaussian noise (WGN) is done to find the transfer function matrix in the discrete-time domain by performing the experiments on the satellite. The accuracy of the identified transfer function is verified using time- and frequency-domain validations. Various MIMO controllers are designed for active vibration isolation in the broadband and the identified corner frequency.

2 The SUITE Hexapod System

2.1 Hardware Configuration. The hardware is composed of two subsystems: a hexapod assembly and a data control system. A hexapod system consists of a moving platform connected to the fixed base through six active struts having one piezoelectric actuator and one geophone sensor on each strut. The piezoelectric actuator is a stack-type actuator with an operational voltage range of −15 to 150 V, an operational stroke length of 30 μm, and resonant frequency at 1.5 kHz. The geophone sensor has a sensitivity of 0.1 V s/mm and a suspension frequency at 12 Hz, above which it acts as a linear velocity sensor with 1 kHz bandwidth. The system consists of two additional triaxial geophone sensors: one attached to a base and the other to a moving platform. As shown in Fig. 1, proof-mass actuators (PMAs) can generate vibrations in the range of 1 to 100 Hz to excite the hexapod system. One proof mass is located on the base plate and the other on the moving platform. Both have a small inclination angle of 5° with the +Z axis of the hexapod.

Each strut consists of a passive isolation stage that provides additional isolation when the active vibration isolation stage fails. The mass of the hexapod suspended payload is 6.2 kg, and the total mass of the hexapod system is 12.6 kg. An electronic data
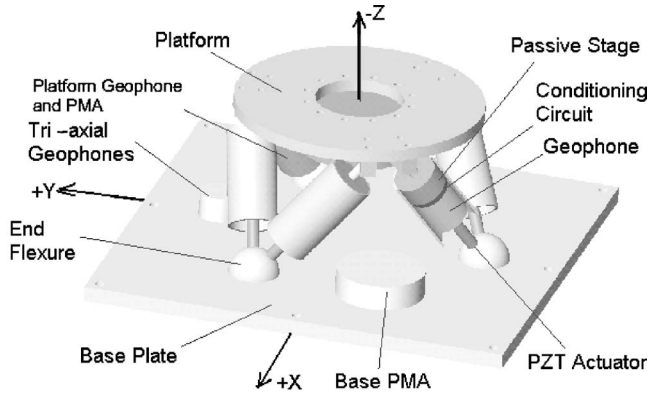
Fig. 1 Perspective view of the 6-DOF SUITE hexapod assembly

control system contains two processors: a 32-bit TMS320C31 digital signal processor (DSP) manufactured by Texas Instruments with 40 MHz clock speed and 20 MIPS (Mega Instructions per Second) execution rate, and a PIC16C74, 8-bit microcontroller manufactured by Microchip. They are used for sampling sensors, driving actuators, computations, and implementing control laws for active vibration isolation.

2.2 Software Architecture. The software for the SUITE is interrupt driven. Nine different interrupt subroutines call programs written in the C language for initialization, control-law implementation, memory release, and clean-up tasks. Out of the existing nine routines, routines 1–3 are used for loading the PMA tables, buzzing the base or the payload, and downloading the data. Routines 4–9 are used for reading values from the tables to actuate the system and to acquire data from geophone sensors. Routines 7–9 are responsible for implementing algorithms for active vibration isolation. Various experimental lists provide methods of initialization and configuration setup before testing starts.

3 Identification of the 6×6 Transfer Function Matrix for Hexapod

Let $\bar{V}_a = [V_{a1} V_{a2} V_{a3} V_{a4} V_{a5} V_{a6}]^T$ be the voltages applied to the six piezoelectric actuators, and $\bar{V}_g = [V_{g1} V_{g2} V_{g3} V_{g4} V_{g5} V_{g6}]^T$ be the voltages measured from six geophone sensors. Equation (1) gives the relation between the voltages applied to the actuators and read from the sensors in the form of a 6×6 transfer function matrix.

$$V_{gi} = f_{ij} V_{aj}, \tag{1}$$

where f_{ij} is the transfer function from the jth input to the ith output channel. The applied test signals and the observed responses were in the form of discrete data, and hence the transfer functions in Eq. (1) were identified in the discrete-time domain. A selection of the sampling rate, test signals, order, and the model structure, design of the experiment, and model validation were the crucial steps in the system identification process. A sampling frequency of 3.5 kHz was selected for all the experiments performed on the satellite. The chirp signal with its frequency content up to 100 Hz and continuously decreasing magnitude from 25 to 5 V and the WGN with frequency contents up to 250 Hz were used as the test signals. The amplitude of each test signal was adjusted so that the saturation of the sensor/actuator was avoided during data acquisition and that the persistent excitation was guaranteed.

The test signals were applied to each strut of the hexapod one at a time, and all the six geophone-sensor data were recorded. The experiment was repeated by applying the same signal to the six struts. 4096 points of chirp input-output signal were used to identify the transfer functions in Eq. (1), using autoregression with exogeneous (ARX) inputs, autoregression moving average with

exogeneous (ARMAX) inputs, and Box–Jenkins (BJ) model structures with orders ranging from three to seven [11].

The fifth-order BJ model structures obtained all 36 transfer functions in Eq. (1) accurately. For example, Eqs. (2) and (3) describe the transfer functions obtained when the input is applied to the first piezoelectric actuator and the output is measured from the first and the second geophone sensor, respectively.

$$f_{11} = \frac{2.174z^4 - 8.646z^3 + 12.9z^2 - 8.552z + 2.126}{z^5 - 2.93z^4 + 2.156z^3 + 1.131z^2 - 2.007z + 0.6512}, \tag{2}$$

$$f_{12} = \frac{0.01(-1.198z^5 + 4.821z^4 - 7.279z^3 + 4.887z^2 - 1.231z)}{z^5 - 2.977z^4 + 1.983z^3 + 1.929z^2 - 2.901z + 0.9652} \tag{3}$$

Model validation in the time and frequency domain was the next step of the system identification. Figure 2 shows the simulated and experimental responses when a 40 Hz sinusoid was applied to the SUITE hexapod. They matched well in the time domain. Figure 3 shows the Bode plot of Eq. (2) and that of the transfer function identified with the bandlimited WGN. They matched well in the [10 Hz, 200 Hz] frequency range that is the WGN bandwidth. Simulated and experimental responses of all the 36 transfer functions matched well in the time and frequency domains, and their order conformed with the order of analytical models derived in [12]. As a part of the identification process, transmissibility of the hexapod platform was identified empirically. The hexapod base was excited using sinusoids of various frequencies up to 100 Hz, and the triaxial geophones located on the base/platform of the hexapod were read. A 35 Hz frequency component was dominantly observed in each experiment and hence considered as one of the corner frequencies for vibration isolation.

4 Multivariable Controller Design

Equation (2) indicates that two low-frequency non-minimum-phase zeros exist in the diagonal transfer functions of the 6×6 transfer function matrix at 0.6488 and 3.5742 Hz limiting the bandwidth of the controller. We set all nondiagonal transfer functions to zero and found non-minimum-phase transmission zeros of the MIMO system. They are located at natural frequencies of 1787.5, 2.2, 3.6, 3.1, 2.4, 0.6, 1.2, and 3.7 Hz. The actual response of the system was not significantly delayed nor in the direction opposite to the input. However, the presence of non-minimum-phase zeros in the model affects the performance in time- and frequency-domain model validation.

When any test signal is applied to a particular actuator, the relative signal magnitudes of the responses from the six geophone sensors indicate the coupling among various input/output channels. It justifies the requirement of multivariable controller augmentation using techniques such as Linear Quadratic Gaussian/Loop Transfer function Recovery (LQG/LTR) and H^∞ control [13]. For MIMO controller designs presented in this section, the plant transfer function matrix is transformed to the continuous-time domain for the ease of calculation and back to the discrete-time domain for the simulation.

4.1 LQG/LTR Controller Design. Equations (4)–(6) give the state-space representation and a control law required for the plant transfer function matrix.

$$\dot{x} = Ax + Bu + L\xi \tag{4}$$

$$y = Cx + \theta \tag{5}$$

$$u = -G_g x \tag{6}$$

where $A^{180 \times 180}$, $B^{180 \times 6}$, and $C^{6 \times 180}$ is a state-space representation of the six-input six-output system with 180 states, and L is the plant noise matrix. ξ and θ are white Gaussian plant and sensor
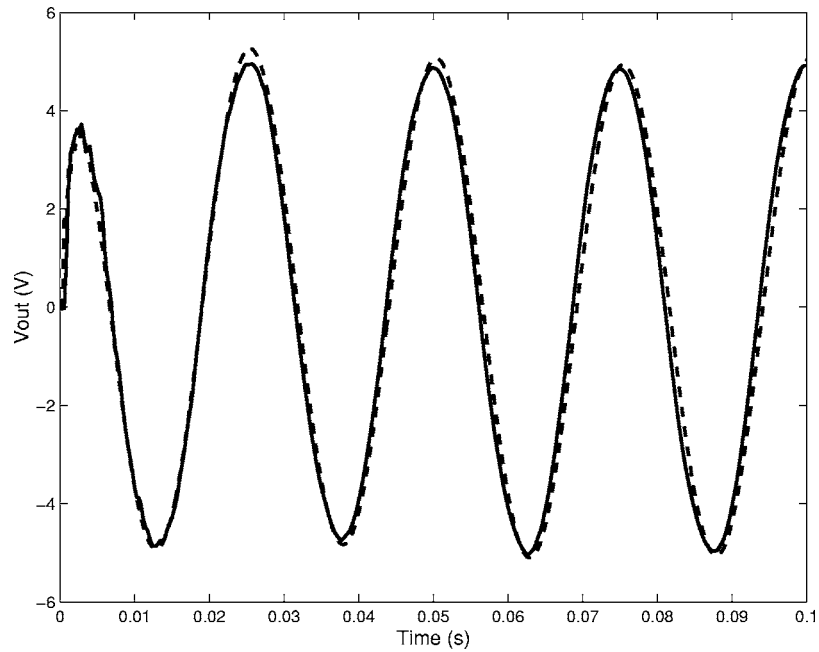
Fig. 2 Simulated (dashed) and experimental (solid) responses to a 40 Hz sinusoid input signal

noises with zero mean and constant intensity covariance matrices ψ and ϕ, respectively. If we assume that $\psi=I$ and $\phi=\mu I$, where I is the identity matrix and μ is the measure of the sensor accuracy, then in the whole design process, μ and L become two design parameters. The μ value was found by reading six sensors without actuating all the six piezoelectric actuators. The mean value (0.01) of the standard deviation of each signal was assigned to μ. Using

the Kalman filter theory, the filter gain matrix H was found. Using the linear quadratic regulator (LQR) theory, the optimal control gain G_g was found to achieve the performance specifications. Continuous-time algebraic Riccati equation (CARE) was used to find both filter and controller gain matrices using their duality. The values are given in Eqs. (7) and (8). These matrices are then used to design the controller (9).
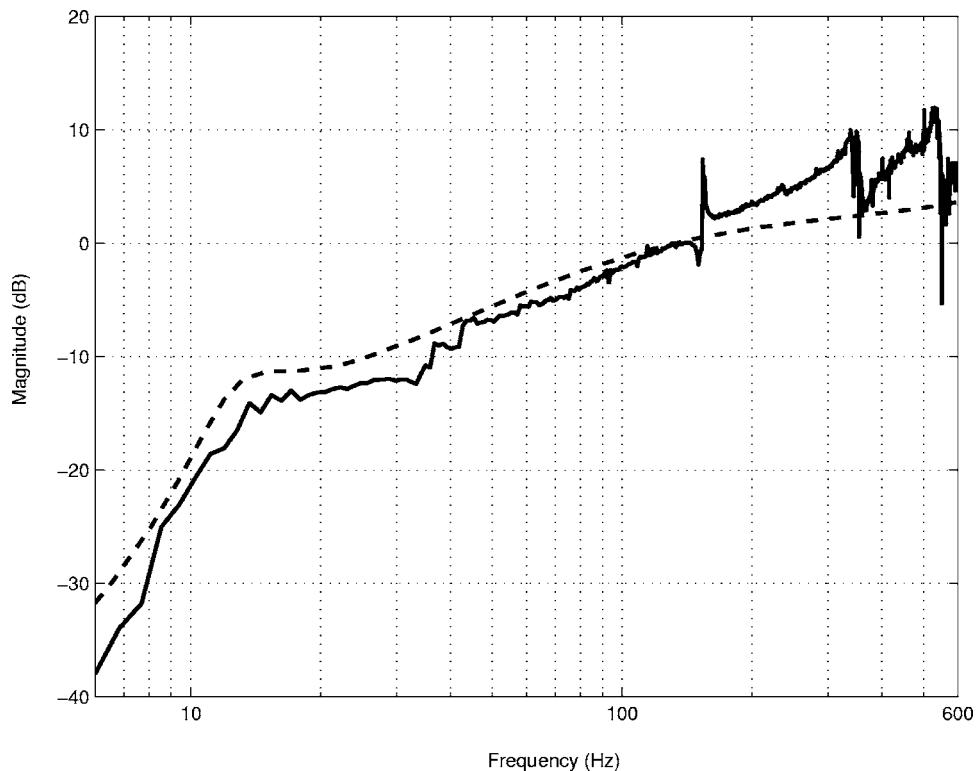

Fig. 3 A comparison of the Bode plots of the transfer functions obtained using system identification (dashed—simulation) and with the WGN (solid—experimental)
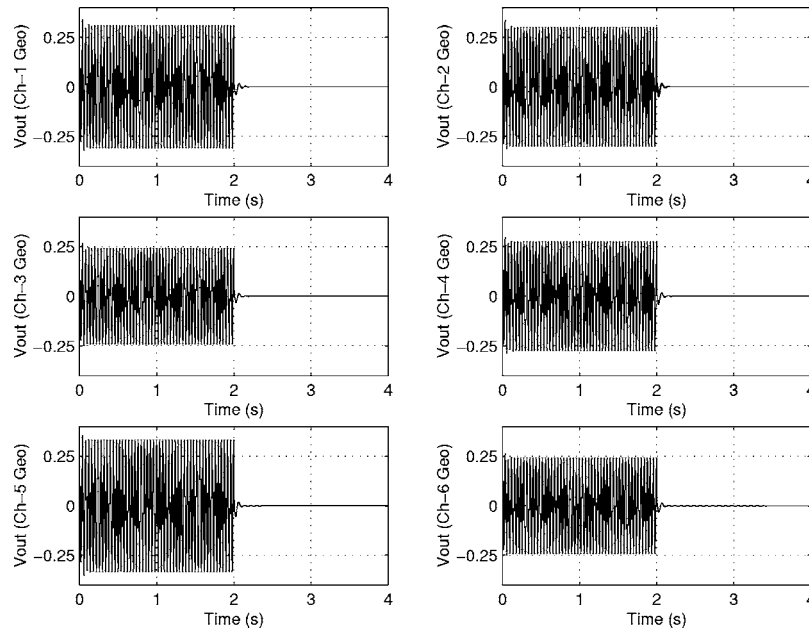
Fig. 4 Simulated responses of all the six channels of LQG/LTR controller to 25 Hz sinusoid used as the plant input disturbance

$$G_g = \begin{bmatrix} 599.1704 & 58.8604 & . & . & 0.0000 \\ -2.1267 & -0.2089 & . & . & -0.0123 \\ 1.7705 & 0.1739 & . & . & 0.0027 \\ 0.2690 & 0.0261 & . & . & -0.0028 \\ -32.9969 & -3.2555 & . & . & 0.0133 \\ 0.0567 & 0.0054 & . & . & 9.6278 \end{bmatrix} \qquad (7)$$

$$H = \begin{bmatrix} 0.9034 & 0.0000 & 0.0000 & 0.0000 & 0.0000 & 0.0000 \\ 0.2519 & 0.0000 & 0.0000 & 0.0000 & 0.0000 & 0.0000 \\ . & . & . & . & . & . \\ . & . & . & . & . & . \\ 0.0000 & 0.0000 & 0.0000 & 0.0000 & 0.0000 & 0.0003 \end{bmatrix} \qquad (8)$$

$$K = G(sI - A + BG + HC)^{-1}H \qquad (9)$$

When a 25 Hz sinusoid of unit amplitude was applied to six channels simultaneously as the plant input disturbance for two seconds in the simulation of this LQG controller, the vibration was effectively attenuated by 13 dB. Figure 4 shows the vibration attenuation in all six channels and the settling of the system after two seconds. In these results of the LQG controller the vibration attenuation up to 100 Hz frequency was not satisfactory. The designed LQG/LTR controller had limited loop-transfer-function recovery due to the presence of the non-minimum-phase zeros in the model.

4.2 H^∞ Controller Design. We expressed the plant transfer function in a lower linear fractional form P, which describes the relation of the exogenous input vector w and the control input vector u with the exogenous output vector z and the measured output vector v. If T_{wz} denotes the transfer function matrix from the exogenous input vector w to the exogenous output vector z, then the H^∞ problem reduces to finding a controller K that will minimize the infinite norm of T_{wz}, maintaining the closed-loop stability. In our control system represented in Fig. 5, the reference input $r(t)$ is the exogenous input w, and the control input $u(t)$ is the control energy input u for the equivalent system. The exogenous output v is defined as $r(t) - y(t)$, and the exogenous output

vector z as the vector $[z_1, z_2]$ containing the weighted error and control signals, respectively. The objective of the design is to minimize the infinite norm of the matrix N given by Eq. (10)

$$N = [W_2 KS \ T \ W_1 S]^T, \qquad (10)$$

where

$$W_1 = \frac{(1000)}{(s + 600)} I^{6\times 6}, \qquad (11)$$

$$W_2 = I^{6\times 6}, \qquad (12)$$

$$S = \frac{1}{1 + GK}, \quad T = \frac{GK}{1 + GK}. \qquad (13)$$

The matrix N is the cost function, and the matrices W_1 and W_2 are the weights for the error signal and the control signal in the cost estimation function, respectively. In this particular case, W_2 is assigned a constant value over the entire frequency range, and W_1 is assigned a higher weight in the lower-frequency range. From the first element of N, the lower magnitude of the W_2 matrix denotes that there is less weight for control input in the minimization of the infinite norm of the matrix KS. The unity value for W_2 is selected in order to relieve the specification constraints on KS. Equation (14) gives the relation between various inputs and
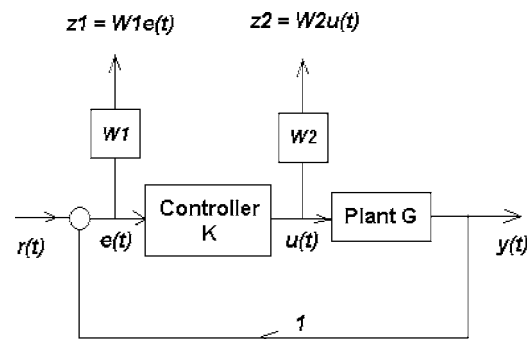

Fig. 5 Block diagram for the weight assignment to the control energy $u(t)$ and error $e(t)$ in the H^∞ controller design
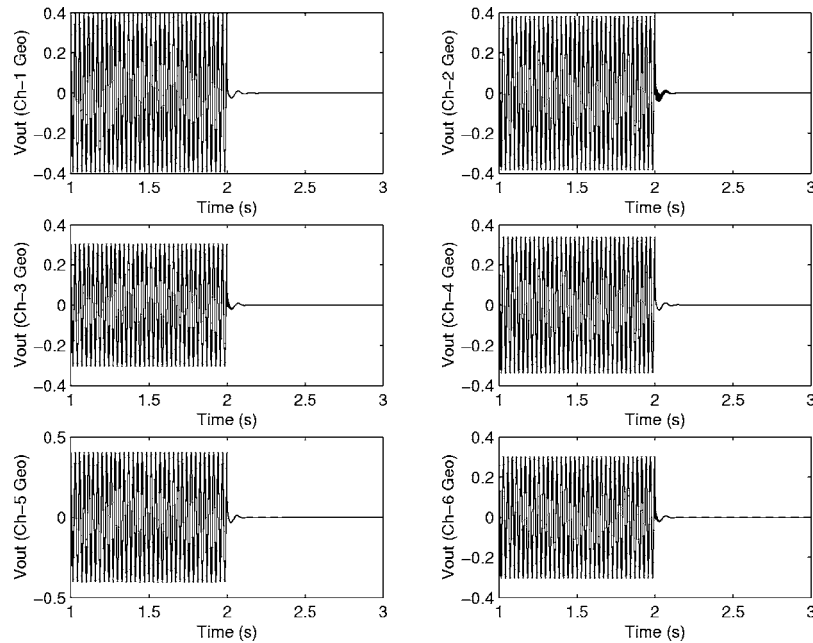
Fig. 6 Simulated responses of all the six channels of the H^∞ controller to a 35 Hz sinusoid used as plant input disturbance

outputs given by lower linear fractional form P of the plant transfer function matrix G.

$$\begin{bmatrix} z \\ v \end{bmatrix} = \begin{bmatrix} z_1 \\ z_2 \\ r-y \end{bmatrix} = \begin{bmatrix} W_1 & -W_1 G \\ 0 & W_2 \\ I & -G \end{bmatrix} \begin{bmatrix} r \\ u \end{bmatrix} = P \begin{bmatrix} w \\ u \end{bmatrix} \qquad (14)$$

We used Eq. (14) for the design of the H^∞ controller using a MATLAB "hinf-syn" command. In the simulation, the H^∞ controller achieved 8 dB vibration attenuation at 35 Hz. Figure 6 shows the vibration attenuation of all six channels and the settling of the system after two seconds when a 35 Hz sinusoid of unit amplitude was applied to all the channels as a plant input disturbance.

5 Conclusions

We modeled the 6-DOF SUITE hexapod assembly to design controllers for vibration isolation. The six-input six-output model of the hexapod was built on the basis of data measured by all the six geophone sensors when the system was excited with a chirp signal and a WGN. Various model structures such as ARX, ARMAX, and BJ were used to build the model.

Using the fifth-order BJ model structure, we identified a 6×6 transfer function matrix for the SUITE hexapod. The nonzero off-diagonal terms in the transfer function matrix denoted the dynamic coupling among various input/output channels. Then we performed the time-domain and frequency-domain model validation to verify the accuracy of the identified transfer function matrix. The experimental and simulated responses matched very well in the time domain for both step inputs and sinusoidal inputs at various frequencies. The Bode plots of the model and the actual transfer functions obtained using the chirp signal and the WGN also matched well in the frequency range of [10 Hz, 200 Hz], which is the effective frequency content of the WGN.

Multivariable controllers to reduce vibration were developed using LQG/LTR and H^∞ controller design techniques. These controllers showed 13 and 8 dB vibration attenuation at 25 and 35 Hz, respectively. There was no specific advantage of using H^∞ over LQG/LTR. The performances of both the controllers were about the same because the non-minimum-phase zeros located at 0.6488 and 3.5742 Hz limited the bandwidth of the controllers.

References

[1] Lauffer, J. P., Hinnerichs, T. D., Kuo, C. P., Wada, B., Ewaldz, D., Winfough, B., and Shankar, N., 1996, "Milling Machine for the 21st Century—Goals, Approach, Characterization and Modeling," Proc. SPIE, **2721**, pp. 326–340.
[2] Warnecke, H. J., Neugebauer, R., and Wieland, F., 1998, "Development of Hexapod Based Machine Tool," CIRP Ann., Manufacturing Technology, **47**, pp. 337–340.
[3] Trucco, R., Pepe, F., and Galeone, P. C., 1996, "Hexapod Pointing System," *Proc. of the 3rd Intl. Conference on Spacecraft Guidance, Navigation and Control Systems*, pp. 201–208.
[4] Pernechele, C., Bortoletto, F., and Reif, K., 1998, "Hexapod Control for an Active Secondary Mirror: General Concept and Test Results," Appl. Opt., **37**, pp. 6816–6821.
[5] O'Brien, J. F. and Neat, G. W., 1995, "Six-Axis Vibration Isolation Technology Applied to Space Interferometers, Spaceborne Interferometry II," Proc. SPIE, **2477**, pp. 9–19.
[6] Nanua, P., Waldron, K. J., and Murthy, V., 1990, "Direct Kinematical Solution of Stewart Platform," IEEE Trans. Rob. Autom., **6**, pp. 483–444.
[7] Watson, L. T., 1988, "Globally Convergent Homotopy Algorithms for Nonlinear Systems of Equations," TR 90-26, Department of Computer Science, Virginia Polytechnic Institute and State University, Blacksburg, VA.
[8] Air Force Research Laboratory, Space Vehicle Directorate, 1999, "Satellite UltraQuiet Isolation Technology Experiment (SUITE)," Guest Investigator's Handbook, Kirtland AFB, Albuquerque, NM.
[9] Anderson, E. H., Fumo, J. P., and Erwin, S. R., 2000, "Satellite Ultraquiet Isolation Experiment (SUITE)," Proc. of IEEE Aerospace Conference, Vol. 4, pp. 299–313.
[10] Geng, J. Z. and Haynes, L. S., 1994, "Six Degree-of-Freedom Active Vibration Control Using the Stewart Platform," IEEE Trans. Control Syst. Technol., **2**, pp. 45–53.
[11] Ljung, L., 1999, *System Identification, Theory for User*, Prentice–Hall, Englewood Cliffs, NJ, Chap. 1, pp. 8–9.
[12] Joshi, A., 2002, "System Identification and Multivariable Control for a Satellite UltraQuiet Isolation Technology Experiment (SUITE)," M.S. thesis, Texas A&M University, College Station.
[13] Jayasuriya, S., 2001, "MEEN 652, Multivariable Control Design," *Class Notes*, Texas A&M University, College Station.